

Lattice Gauge Theory[†]

Hartmut Wittig

Theoretical Physics, Oxford University, 1 Keble Road, Oxford OX1 3NP, UK

Abstract

The status of lattice calculations in Quantum Field Theory is reviewed. A major part is devoted to recent progress in formulating exact chiral symmetry on the lattice. Another topic which has received a lot of attention is the influence of dynamical quark effects. Attempts to quantify these effects for the light hadron spectrum and flavour singlet amplitudes are discussed, as well as other expected qualitative features of simulations with dynamical quarks. The remaining parts of the review include recent results for the light quark masses using non-perturbative renormalisation and the spectrum of glueballs and heavy hybrids computed using anisotropic lattices.

1. Introduction

Since Wilson's original formulation of lattice gauge theories in 1974 [1], lattice methods have developed into a mature area of research with a wide range of applications, including subjects as diverse as QCD, Higgs models and Quantum Gravity. It is therefore quite impossible to cover all recent activities in Lattice Gauge Theory in a single review. Therefore, I shall concentrate on lattice QCD applied to the calculation of hadron masses and the evaluation of weak matrix elements. Another subject which I shall present in detail, and which has received a lot of attention recently, is the lattice formulation of chiral symmetry. Indeed, over the past two years it has emerged that chiral gauge theories can be put on the lattice in a consistent way, something which has been thought to be impossible for a long time. These new developments have wide-ranging implications for a large class of theories, which clearly merits a detailed discussion.

An overview of those areas which will *not* be discussed here can be found in the proceedings of recent annual conferences on Lattice Field Theory. In particular, I refer the reader to the plenary talks on

- QCD at finite temperature and density [2–4]
- The electroweak phase transition [5–7]
- Topology and confinement [8,9]
- Lattice gravity and random surfaces [10, 11]

Furthermore there are reviews of lattice gauge theory given at recent conferences on High Energy Physics [12,13].

[†] Plenary talk presented at International Europhysics Conference on High-Energy Physics (EPS-HEP 99), Tampere, Finland, 15–21 July 1999.

1.1. General remarks

Many of the concepts and techniques of Lattice Gauge Theories can be easily introduced in the context of QCD. Here, the lattice formulation provides a non-perturbative framework to compute relations between Standard Model parameters and experimental quantities from first principles.

The discretisation is achieved by introducing a euclidean space-time lattice with spacing a and volume $L^3 \cdot T$. The inverse lattice spacing, a^{-1} acts as an UV cutoff, which preserves the gauge invariance of the theory. The quark and antiquark fields $\psi(x), \bar{\psi}(x)$ are associated with the lattice sites x , whereas the gauge field is represented by the so-called link variable $U_\mu(x)$, which connects neighbouring lattice sites, and is an element of the gauge group SU(3). After choosing suitable discretisations of the Yang-Mills action S_G and the quark action S_F , the expectation value of an observable Ω is defined as

$$\langle \Omega \rangle = \frac{1}{Z} \int \prod_{x,\mu} dU_\mu(x) \int \prod_x d\bar{\psi}(x) d\psi(x) \Omega e^{-S_G - S_F} \quad (1)$$

and the functional integral Z is determined by requiring $\langle 1 \rangle = 1$. The discretisation procedure has hence given a meaning to the functional integral measure, which becomes a simple product measure. More importantly, after integrating out the quarks this formulation allows for a *stochastic* evaluation of $\langle \Omega \rangle$ using Monte Carlo techniques.

Ideally one would like to use lattice QCD as a phenomenological tool. A typical application would be, for instance, the computation of the strange quark mass $m_s^{\overline{\text{MS}}}(2 \text{ GeV})$, using the kaon mass, m_K and the pion decay constant as input parameters. However, as I shall explain below, *realistic* simulations of lattice QCD are difficult.

The first problem one has to address are lattice artefacts (cutoff effects). Let Ω denote the quantity we wish to compute on the lattice, e.g. a hadron mass. Then the expectation values on the lattice and in the continuum differ by corrections of order a^p , viz

$$\langle \Omega \rangle^{\text{lat}} = \langle \Omega \rangle^{\text{cont}} + O(a^p), \quad (2)$$

where the power p in the correction term depends on the chosen discretisation of the QCD action. Values of a which can currently be simulated lie in the range $a \approx 0.2 - 0.05 \text{ fm}$. The size of the correction term can in some cases be as large as 20%, depending on the quantity and the chosen discretisation. It is then clear that an extrapolation to the continuum, $a \rightarrow 0$ is required in order to obtain the desired result. This extrapolation can be much better controlled if the chosen discretisation avoids small values of p .

Perhaps the biggest challenge as far as lattice QCD is concerned, is the inclusion of dynamical quark effects. After integrating out the quark fields the expression for the expectation value reads

$$\langle \Omega \rangle = \frac{1}{Z} \int \prod_{x,\mu} dU_\mu(x) \prod_f \det(D + m_f) \Omega e^{-S_G}, \quad (3)$$

where D is the lattice Dirac operator and m_f is the mass of quark flavour f . The evaluation of the determinant in eq. (3) in numerical simulations is still very costly, even on today's massively parallel computers. In many applications the determinant has therefore been set to 1. This defines the so-called *quenched approximation*, which corresponds to neglecting quark loops in the evaluation of $\langle \Omega \rangle$. Although this represents a rather drastic assumption about the influence of quark-induced quantum effects, the quenched approximation works surprisingly well, as I shall describe later.

An indirect consequence of using the quenched approximation is the observed *scale ambiguity*. That is, the calibration of the lattice spacing in physical units, $a^{-1} [\text{MeV}]$, is dependent on the quantity Q which is used to set the scale

$$a^{-1} [\text{MeV}] = \frac{Q [\text{MeV}]}{(aQ)}, \quad Q = f_\pi, m_\rho, \dots \quad (4)$$

This ambiguity arises because different quantities Q are affected by quark loops in different ways.

There are also restrictions on the quark masses m_q that can be simulated. In general the following inequalities should be satisfied

$$a \ll \xi \ll L, \quad (5)$$

where L is the spatial extent of the lattice volume. The quantity ξ denotes the correlation length of a

typical hadronic state, which serves as a measure of the quark mass. The inequality on the right places restrictions on the light quark masses that can be simulated: if those are too light one may suffer from finite-size effects, since ξ becomes large. Typical spatial extensions of $L \approx 1.5 - 3 \text{ fm}$ imply that the physical pion mass cannot be reached. The left inequality restricts the masses of heavy quarks. Since $a^{-1} \approx 2 - 4 \text{ GeV}$, it is clear that relativistic b -quarks cannot be simulated. One therefore relies on extrapolations in m_q to connect to the physical u , d and b quarks. Obviously it is of great importance to control such extrapolations.

Finally there is the issue of chiral symmetry breaking. A famous no-go theorem by Nielsen and Ninomiya [14] implies that under fairly mild assumptions exact chiral symmetry cannot be realised at non-zero lattice spacing. Therefore, the chiral and continuum limits cannot be separated. For many (but not all) applications of lattice QCD this may not be a severe limitation, but the no-go theorem has so far precluded all attempts to achieve a realistic lattice formulation of the electroweak sector of the Standard Model.

1.2. Outline

The remainder of this article is as follows: section 2 deals with the properties of lattice Dirac operators: it is described how lattice artefacts in observables can be successfully reduced by constructing “improved” lattice actions. The major part of section 2 is devoted to recent developments which have ultimately led to the construction of lattice chiral gauge theories with exact gauge invariance. Section 3 discusses recent simulations of QCD with dynamical quarks. Results which quantify sea quark effects in the light hadron spectrum are presented, and moreover the qualitative effects of sea quarks in flavour-singlet amplitudes and regarding the breakdown of linear confinement (“string breaking”) are discussed. In section 4 recent results for the light quark masses are presented. Progress in this area has been achieved through the non-perturbative matching of lattice results to the $\overline{\text{MS}}$ scheme. In section 5 I describe recent results for the spectrum of glueballs and heavy hybrids. Section 6 contains a brief overview of results for some weak hadronic matrix elements which could not be reviewed extensively due to lack of time. Finally, a summary is presented in section 7.

2. The lattice Dirac operator

This section deals with the general properties of lattice fermions. After recalling the fermion doubling

problem we shall discuss the implementation of the Symanzik on-shell improvement programme, which systematically reduces lattice artefacts in physical observables and thus makes extrapolations to the continuum limit more reliable. The main part of this section, however, reviews the recent progress made in formulating chiral symmetry on the lattice.

2.1. Fermion doubling revisited

Suppose we want to describe massless *free* fermions on the lattice. The lattice action can be written as

$$S_F = a^4 \sum_{x,y} \bar{\psi}(x) D(x-y) \psi(y), \quad (6)$$

where D denotes the lattice Dirac operator. In particular, one would like to formulate the theory such that D satisfies the following conditions

- (a) $D(x-y)$ is local
- (b) $D(p) = i\gamma_\mu p_\mu + O(ap^2)$
- (c) $D(p)$ is invertible for $p \neq 0$
- (d) $\gamma_5 D + D \gamma_5 = 0$

Locality is required in order to ensure renormalisability and universality of the continuum limit; it ensures that a consistent field theory is obtained. Furthermore, condition (c) ensures that no additional poles occur at non-zero momentum. If this is not satisfied, as is the case for the “naïve” discretisation of the Dirac operator, additional poles corresponding to spurious fermion states can appear: this is the famous fermion doubling problem. Finally, condition (d) implies that S_F is chirally invariant.

The main conclusion of the Nielsen-Ninomiya no-go theorem is that conditions (a)–(d) cannot be satisfied simultaneously. Since one is not willing to give up locality and condition (b), this implies that one is usually confronted with the choice of tolerating either doubler states or explicit chiral symmetry breaking. This is manifest in the two most widely used lattice fermion formulations: staggered (“Kogut-Susskind”) fermions leave a chiral $U(1)$ subgroup invariant, but only partially reduce the number of doubler species [15]. Wilson fermions, on the other hand, remove the doublers entirely at the expense of breaking chiral symmetry explicitly. This is easily seen from the expression for the free Wilson-Dirac operator

$$D_W^{(0)} = \frac{1}{2} \gamma_\mu (\nabla_\mu + \nabla_\mu^*) - \frac{1}{2} a \nabla_\mu^* \nabla_\mu. \quad (7)$$

Using the definitions for the forward and backward lattice derivatives, ∇_μ and ∇_μ^* , one easily proves conditions (a)–(c), while it is obvious that (d) is not

satisfied. Nevertheless, the (interacting) Wilson-Dirac operator D_W is widely used in simulations of lattice QCD. This is because chiral symmetry breaking in a vector-like theory is often merely an inconvenience, but no fundamental obstacle.

2.2. Improved discretisations of the Wilson action

Another consequence of using the Wilson-Dirac operator is the presence of large cutoff effects in physical observables. One can show that the leading lattice artefacts are of order a (i.e. $p = 1$ in eq. (2)), while e.g. for staggered fermions the lattice corrections start at order a^2 .

It is important to realise the definition of a lattice action is not unique: one can add any number of operators which formally vanish in the continuum limit, provided that they comply with the correct symmetry and locality requirements. Given this relative freedom in defining lattice actions, an obvious question is whether one can find *improved* discretisations for lattice fermions, for which the cutoff effects are reduced. Two approaches have been the subject of much recent activity. One is based on the Symanzik improvement programme [16, 17], in which lattice artefacts are removed order by order in the lattice spacing. In the second approach one seeks to construct a “perfect” lattice action (which is essentially free of lattice artefacts), using renormalisation group techniques [18].

Sheikholeslami and Wohlert have shown that in QCD with Wilson fermions the Symanzik improvement programme can be implemented to lowest order in a by adding one dimension-5 counterterm to D_W . The resulting operator (with bare mass m_0) reads

$$D_{SW} = D_W + m_0 + \frac{ia}{4} c_{sw} \sigma_{\mu\nu} F_{\mu\nu}, \quad (8)$$

where $F_{\mu\nu}$ is a lattice transcription of the field tensor. In order to remove all lattice artefacts of order a in hadron masses, the improvement coefficient c_{sw} has to be fixed by imposing a suitable improvement condition. Such a condition is provided by requiring that the restoration of the axial Ward identity holds up to terms of order a^2 [20]. It has been applied to determine c_{sw} non-perturbatively for a large range of couplings for both quenched QCD [21, 22] and also for $n_f = 2$ flavours of dynamical quarks [23].

In order to compute matrix elements of local composite operators such as vector and axial vector currents, one has to consider their correctly normalised and improved versions. For instance,

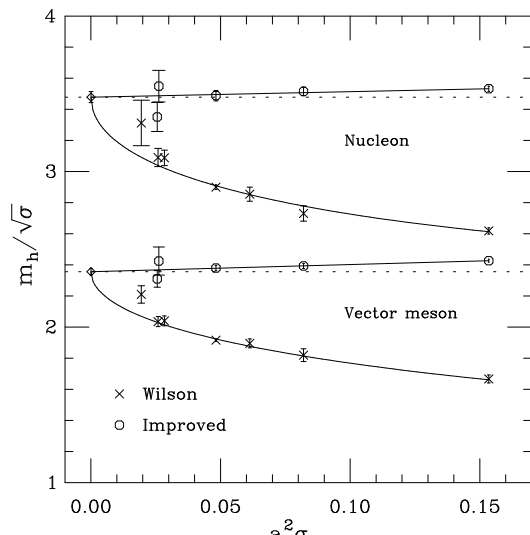


Figure 1. Scaling plot for masses in the vector meson and nucleon channels for improved (circles) and unimproved (crosses) Wilson fermions [22]. The linearity of the data computed with the improved action demonstrates the expected scaling behaviour.

the renormalised axial current $(A_R)_\mu$ in the $O(a)$ improved theory reads

$$(A_R)_\mu = Z_A(1 + b_A a m_q) \{A_\mu + c_A a \partial_\mu P\} \quad (9)$$

where b_A and c_A are improvement coefficients, P is the pseudoscalar density, and Z_A is the renormalisation constant for the axial current. In refs. [21, 24] c_A and Z_A have been determined non-perturbatively, and a general strategy to determine the improvement coefficients and renormalisation constants of all quark bilinears in the $O(a)$ improved theory has been presented in [25]. Detailed studies of the matrix elements of such operators with much better controlled lattice artefacts should therefore soon be feasible.

The remaining question is whether non-perturbative $O(a)$ improvement can be *verified*, in the sense that physical observables computed in the $O(a)$ improved theory can be shown to approach their continuum limit with a rate proportional to a^2 [26]. Detailed scaling studies performed in the quenched approximation have shown that this is indeed the case for meson and baryon masses [22], as well as for matrix elements of vector and axial vector currents [27]. An example is shown in Fig. 1, taken from ref. [22].

In ref. [28] the Symanzik improvement programme was extended to higher orders. The many relevant improvement coefficients have been determined in (mean-field improved [29]) perturbation

theory. $O(a)$ improvement has also been studied for the anisotropic Wilson action [30], for which the temporal and spatial lattice spacings are chosen differently. This offers an advantage in the computation of heavy states, and we will return to this point in section 5.

Another method to construct a lattice action with improved scaling behaviour was presented in ref. [31]. The idea is to use the operator D_{SW} in eq. (8) on smoothed gauge configurations. Such configurations are obtained through a blocking procedure applied to spatial link variables as described in [32]. The resulting action is called the “fat-link” clover action. In a series of papers [33, 34] it has been shown that fat-link clover actions exhibit good chiral properties: the additive renormalisation of the quark mass encountered for Wilson fermions is small (yet non-vanishing), and the renormalisation factors Z_A and Z_V of axial and vector currents are close to unity. Furthermore, scaling tests of various hadron masses have been carried out to test whether cutoff effects of order a have been eliminated.

One concludes that improved discretisations of the Wilson actions are successful and play an ever more important rôle in calculations of the hadron spectrum and matrix elements. Their main advantage is that more accurate results in the continuum limit are obtained. It is important to keep in mind, though, that improved discretisations obtained through the Symanzik improvement programme and also the fat-link clover actions do not alleviate the problem of explicit chiral symmetry breaking.

2.3. Exact chiral symmetry on the lattice

A lot of progress has been made recently in the formulation of chiral fermions on the lattice. In fact, it has been shown how lattice chiral gauge theories can be formulated in a way which preserves locality and gauge invariance. Many new developments in this field have followed the rediscovery of the Ginsparg-Wilson relation [35]

$$\gamma_5 D + D \gamma_5 = a D \gamma_5 D. \quad (10)$$

The significance of this relation had not been realised for a long time, since no non-trivial expression for a Dirac operator D satisfying eq. (10) was known. It is remarkable that two constructions of such a solution have been developed independently at around the same time.

The first goes back to Kaplan’s proposal to realise chiral fermions in the domain wall fermion approach [36]. This was subsequently re-cast by Narayanan and Neuberger, who developed the

“overlap” representation of the chiral determinant [37,38]. Furthermore, Shamir and Furman [39] used a variant of Kaplan’s work to derive the domain wall fermion formulation for vector-like theories like QCD [39]. The second solution to eq. (10) was constructed in the perfect action approach mentioned earlier.

Here I will briefly discuss some of the concepts and applications. More details can be found in recent reviews on Domain Wall fermions [40] and the construction of lattice chiral gauge theories [41, 42].

I shall first discuss the Domain Wall (DW) fermion formulation as described in ref. [39]. The basic idea, proposed in [36] is to introduce an extra (fifth) dimension and to consider fermions coupled to a mass defect in the extra dimension. To make this more explicit, let x, y denote 4-dim. coordinates and s, s' the coordinates in the 5th dimension, which has finite length N_s . The gauge fields are trivial in the 5th direction, and the Dirac operator then has the form

$$D_{ss'}^{\text{DWF}}(x, y) = D^{\parallel}(x, y)\delta_{ss'} + \delta(x - y)D_{ss'}^{\perp} \quad (11)$$

where $D^{\parallel}(x, y)$ is the usual Wilson-Dirac operator with a *negative* mass term, $-M$. The operator $D_{ss'}^{\perp}$ couples fermions in the extra dimension and contains the Dirac mass m . It can now be shown that for $m = 0$ and in the limit $N_s \rightarrow \infty$ there are no fermion doublers and, more importantly, chiral modes of opposite chirality are trapped in the 4-dim. domain walls at $s = 1, N_s$. The physical, 4-dim. fields defined by

$$\begin{aligned} q(x) &= P_R\psi_1(x) + P_L\psi_{N_s}(x) \\ \bar{q}(x) &= \bar{\psi}_{N_s}(x)P_R + \bar{\psi}_1(x)P_L \end{aligned} \quad (12)$$

satisfy exact, continuum-like axial Ward identities at non-zero values of a for $N_s \rightarrow \infty$. This result, derived in [39], formally establishes the correct chiral properties of the lattice regularised theory.

In a real simulation one has to work at finite N_s so that the decoupling of chiral modes is not exact. It is possible to show, however, that the terms which break the chiral symmetry are exponentially suppressed. This point can be illustrated by discussing the relation between the pion mass and the quark mass in Domain Wall QCD. At finite a one has

$$(am_{\pi})^2 = C(am + ae^{-\gamma N_s}), \quad (13)$$

where C is a constant, m is the Dirac mass which appears in D^{\perp} , and $\gamma > 0$. This expression shows that in the limit $N_s \rightarrow \infty$ the bare quark mass is only multiplicatively renormalised (i.e. there is no

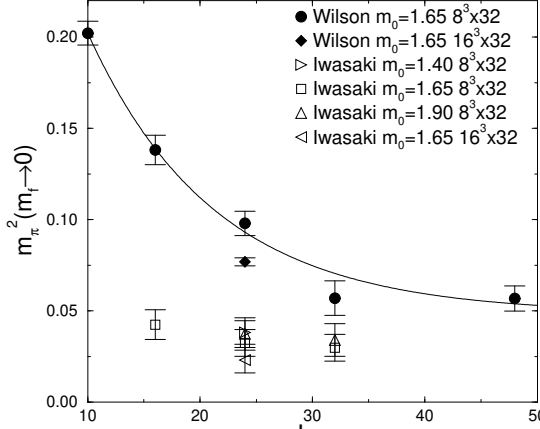


Figure 2. The pion mass in the chiral limit plotted versus the size of the 5th dimension from ref. [43]. Solid circles are the data obtained using the Wilson plaquette action for the gauge field, whereas open symbols denote data obtained using an improved gauge action (Iwasaki). The solid line is a fit assuming $(am_{\pi})^2 = A + B \exp(-\gamma N_s)$, which yields a non-vanishing intercept of $A = 0.048(9)$ in the limit $N_s \rightarrow \infty$ (notation translates as: $L_s \rightarrow N_s, m_0 \rightarrow M, m_f \rightarrow m$).

additive quark mass renormalisation as for ordinary Wilson fermions). It also shows that for finite a there is a residual pion mass in the chiral limit proportional to $a \exp(-\gamma N_s)$.

Hence, the Domain Wall formulation of QCD offers a method to realise almost exact chiral invariance at non-zero lattice spacing at the expense of simulating a 5-dim. theory. An important feature is that lattice artefacts of order a are exponentially suppressed at finite N_s . In other words, the theory is $O(a)$ improved for $N_s \rightarrow \infty$, with exponentially small $O(a)$ corrections expected at finite N_s . As in the case of non-perturbative $O(a)$ improvement the expected improved scaling behaviour in Domain Wall QCD must be verified.

The question that arises is how small a value of N_s one can get away with in order to realise chiral symmetry whilst keeping the computational overhead of simulating an extra dimension at a minimum. In refs. [43, 44] systematic studies of the N_s -dependence of $(am_{\pi})^2$ in the chiral limit have been presented. An example of such an analysis is shown in Fig. 2 [43]. The main conclusion is that the suppression of the residual pion mass expected according to eq. (13) is very slow. At present it is not even clear that it vanishes at all in the limit $N_s \rightarrow \infty$. Further studies, clarifying the rôle of conventional, 3-dim. finite-size effects and the effects of quenching, are required to settle this issue.

There are already extensive numerical studies of physical observables using DW QCD. Results

include studies of QCD thermodynamics [45], weak interaction matrix elements such as those relevant for kaon physics, i.e. the B -parameter B_K and ϵ'/ϵ [46–48] and determinations of the light quark masses [49, 50].

Turning now to the question of constructing chiral gauge theories on the lattice with exact gauge invariance, let us recall that a central ingredient in the construction of such theories is the Ginsparg-Wilson (GW) relation eq.(10), which replaces the condition $\{\gamma_5, D\} = 0$. One key observation, made in [51], is that any lattice Dirac operator satisfying the GW relation has chiral zero modes and satisfies an exact index theorem. It was subsequently realised [52] that the GW relation implies an exact symmetry of the associated action, with infinitesimal variations proportional to

$$\begin{aligned}\delta\psi &= \gamma_5(1 - \tfrac{1}{2}aD)\psi \\ \delta\bar{\psi} &= \bar{\psi}(1 - \tfrac{1}{2}aD)\gamma_5.\end{aligned}\quad (14)$$

Moreover, this symmetry reproduces the correct chiral anomaly in the flavour singlet case. That is, all the hallmarks of the correct chiral behaviour are present in the lattice theory: chiral zero modes, an exact index theorem and the chiral anomaly derived from the Ward identities associated with the exact symmetry.

At this stage left- and right-handed fermions are easily introduced. Furthermore, starting from a solution to the GW relation, it is possible to construct abelian chiral gauge theories on the lattice, which comply with all basic requirements, including exact gauge invariance [53]. The construction extends to the non-abelian case [54], and although a few properties have yet to be established with the same rigour as for abelian theories, there is little doubt that the construction is valid.

An operator which satisfies the GW relation can be constructed in the framework of the overlap formalism. After Kaplan's proposal and independent related work by Frolov and Slavnov [55], Narayanan and Neuberger obtained an expression for the chiral determinant, which is usually termed the “overlap” [37, 38]. Among many other things the overlap was shown to reproduce the correct chiral properties in vector-like theories like QCD [38]. Furthermore, it can be brought into a more manageable expression in terms of a relatively simple lattice Dirac operator D_N . It is defined by [56]

$$\begin{aligned}D_N &= \tfrac{1}{2}\left(1 - X(X^\dagger X)^{-1/2}\right) \\ X &= 1 - D_W,\end{aligned}\quad (15)$$

where D_W is the massless Wilson-Dirac operator. D_N can easily be shown to satisfy the GW relation [57]. Moreover, it was demonstrated that the construction of D_N from the overlap could be reversed, using only the GW relation and factorisation [58].

The obvious question at this point is whether the correct chiral properties of operators satisfying the GW relation can be verified in lattice simulations. A possible strategy is then to check whether the expected global anomalies are exhibited. One example is Witten's observation [59] that SU(2) gauge theory coupled to a single left-handed fermion is mathematically inconsistent. Restricting the discussion to the continuum theory for the moment, this is easily seen by examining the functional integral for this theory after the Weyl fermions have been integrated out, viz

$$\mathcal{Z} = \int [dA] (\det D[A])^{1/2} e^{-S_G[A]}. \quad (16)$$

Here, A is the SU(2) gauge field, and D denotes the Weyl operator. Obviously a sign ambiguity arises due to the presence of the square root in eq.(16). Indeed, for SU(2) there exist non-trivial gauge transformations $g(x)$ which cannot be deformed continuously to the identity, and for which

$$(\det D[A])^{1/2} = -(\det D[A^g])^{1/2}, \quad (17)$$

where A^g denotes the transformed gauge field. This result implies that expectation values defined through \mathcal{Z} are indeterminate, i.e. $\langle \Omega \rangle = “0/0”$.

Although A_μ and A_μ^g are not connected via some smooth gauge transformation, they are none the less connected in the space of gauge fields. Thus, one can define a curve which smoothly interpolates between A_μ and A_μ^g , given by

$$A_\mu(t) = (1 - t)A_\mu + tA_\mu^g, \quad t \in [0, 1]. \quad (18)$$

By invoking the Atiyah-Singer index theorem, Witten showed that the number of eigenvalues of the Dirac operator which cross zero is odd. This observation about the behaviour of the spectral flow along the curve $A_\mu(t)$ then gives rise to the sign ambiguity and hence the mathematical inconsistency. It is now interesting to investigate whether the expected spectral flow can be reproduced on the lattice.

Initially this has been investigated by Neuberger [60]. Then, in ref. [61], Bär and Campos reported on the computation of the eigenvalues of the overlap operator D_N in a lattice simulation along the path which smoothly connects a constant gauge configuration to its gauge transform as in eq.(18).

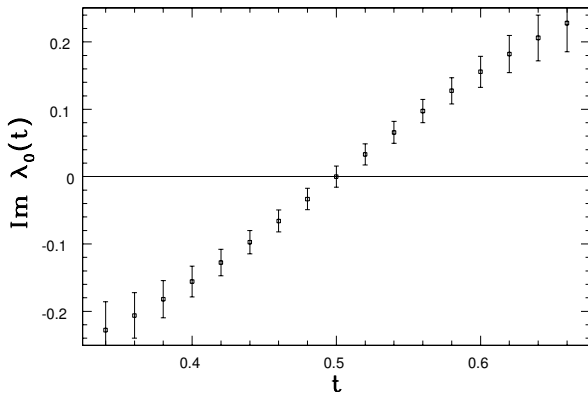


Figure 3. Level crossing for the imaginary part of the lowest eigenvalue of the overlap operator

Focussing on the six lowest eigenvalues they found that only one, i.e. the smallest, λ_0 , becomes zero at $t = 0.5$. The hermiticity properties of D_N imply that one expects the level crossing to occur for the imaginary part of this eigenvalue. Figure 3 demonstrates that the crossing is indeed observed for $\text{Im } \lambda_0$. This result represents a numerical proof of Witten's original argument and is only possible if the lattice Dirac operator has the correct chiral properties. The above example illustrates the enormous progress that has been achieved in the formulation of chiral symmetry.

Other recent work in this area includes investigations of spontaneous chiral symmetry breaking [62–64], the locality properties of D_N [65] and the development of efficient implementations of Ginsparg-Wilson fermions [66–70].

In view of these results it should be clear now that a consistent formulation of the Standard Model exists beyond perturbation theory. There are also important consequences for future lattice studies of supersymmetric models: in many ways the intrinsically supersymmetric features in such models bear resemblance to the rôle of chiral symmetry in QCD.

3. Simulations with dynamical quarks

Now we turn to discuss the other great challenge in present simulations of QCD, namely the inclusion of dynamical quark effects. As mentioned in section 1.1 the quenched approximation is still widely used for many phenomenologically interesting quantities, and in order to enhance the predictive power of lattice simulations it is of great importance to assess the influence of dynamical quarks.

Before such an assessment can be made with the required accuracy, it is necessary to perform precise calculations of experimentally known quantities in the quenched theory. Such benchmarks serve not only to detect significant effects due to dynamical quarks, but also illustrate how closely the quenched approximation resembles the real world.

3.1. Quenched light hadron spectrum

The CP-PACS Collaboration recently presented a precision calculation of the light hadron spectrum in quenched QCD using the (unimproved) Wilson action [71], which superseded earlier studies by GF11 [72]. The findings of CP-PACS are summarised in the plot shown in Fig. 4. Although the qualitative features of the spectrum are well reproduced by the quenched lattice data, one finds significant deviations from the experimentally observed spectrum. For instance, the ratio of the nucleon and ρ masses is calculated as

$$m_N/m_\rho = 1.143 \pm 0.033, \quad (19)$$

which is 6.7% (2.5 σ) below the experimental value of 1.218. Similarly, vector-pseudoscalar mass splittings such as $m_{K^*} - m_K$ are too small by 10 – 16% (4 – 6 σ), depending on whether m_K or m_ϕ is used as input to fix the strange quark mass. This result implies that, for the first time, a *significant* deviation between the quenched QCD spectrum and nature is detected. The main conclusion of ref. [71] is that quenched QCD describes the light hadron spectrum at the level of 10%. However, it also shows that the quenched approximation works surprisingly well, since the discrepancy is fairly mild. This has important consequences for other, phenomenologically more interesting quantities, for which one may be stuck with the quenched approximation for some time to come.

Although the CP-PACS results represent a real benchmark in terms of statistics, parameter values and lattice volumes, further corroboration of these findings is still required. It should be added that the results depend crucially on the modelling of the quark mass dependence of observables. Usually the results of Chiral Perturbation Theory can be used to guide the extrapolations in the quark masses. However, in the quenched approximation one expects deviations from the predictions of Chiral Perturbation Theory due to the appearance of “quenched chiral logarithms” [74, 75], which makes the extrapolation of hadron masses close to the chiral limit hard to control. Furthermore, the CP-PACS results were obtained using unimproved Wilson fermions which have large lattice artefacts.

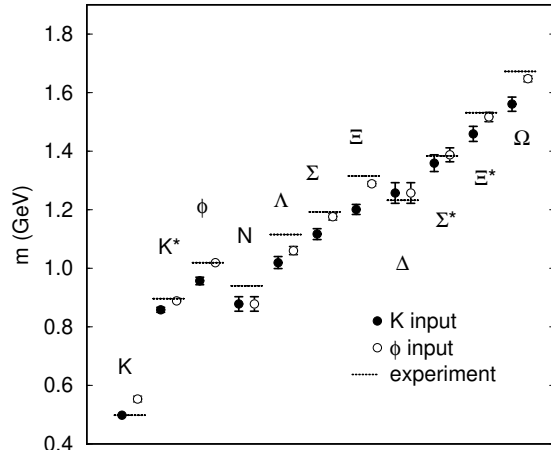


Figure 4. The quenched hadron spectrum from ref. [71] compared to experiment (dashed lines).

It is therefore desirable to check whether the extrapolations to both the chiral and continuum limits are controlled.

Recent calculations employing different discretisations have largely confirmed the findings of [71]: the MILC Collaboration [76] has used staggered fermions and finds a value for the nucleon to rho mass ratio in the continuum limit of

$$m_N/m_\rho = 1.254 \pm 0.018 \text{ (stat)} \pm 0.028 \text{ (syst)}, \quad (20)$$

This is in broad agreement with experiment, but the difference to the CP-PACS result amounts to only two σ . A recent calculation by UKQCD using $O(a)$ improved Wilson fermions [77] essentially confirms the conclusion of CP-PACS, namely that the quenched light hadron spectrum agrees with experiment at the level of 10 %.

3.2. Light hadron spectrum for $n_f = 2$

An obvious question is whether sea quark effects can account for the observed deviation of the quenched light hadron spectrum from experiment. Before discussing some results it is useful to explain a few technical issues which are relevant for simulations with dynamical quarks.

First it is evident that improved lattice actions have an even more important rôle to play. Since simulations with dynamical quarks are very expensive, one cannot afford to control the extrapolation to the continuum limit by simulating very small lattice spacings, whilst keeping sufficiently large spatial volumes in physical units. In order to be able to separate sea quark effects from lattice artefacts, it is vital to

Table 1. Recent simulations with $n_f = 2$ flavours of dynamical quarks, together with the sustained computer power (in GFlops). The other two columns denote the choice of discretisation for the gauge action S_G and the Dirac operator used in S_F .

Collab.	GFlops	S_G	S_F
RBC	~ 250	Plaq.	D^{DWF}
CP-PACS	~ 300	Iwasaki	D_{SW} , tad.
UKQCD	~ 30	Plaq.	D_{SW} , n.p.
SESAM/T χ L	~ 14	Plaq.	D_W
MILC	$\gtrsim 7$	LW	D_{stag}

have control over the latter. Details of recent simulations with $n_f = 2$ flavours of dynamical quarks are listed in Table 1. The quark actions used in these calculations are based on the $O(a)$ improved Wilson-Dirac operator D_{SW} (using either the non-perturbative determination for c_{sw} or its estimate in mean-field improved perturbation theory), the unimproved operator D_W , domain wall quarks or staggered fermions. In addition to the widely used plaquette action for the gauge fields (labelled ‘‘Plaq.’’ in Table 1), two collaborations also use improved gauge actions. Such actions were introduced by Lüscher and Weisz [78] and Iwasaki [79]: they have been found to lead to smaller lattice artefacts in the static quark potential, although the bulk of the discretisation effects in hadronic quantities can only be reduced by employing improved fermion actions [80].

The two flavours of (degenerate) dynamical quarks with mass m^{sea} are usually identified with the physical u and d quarks. Unlike in the real world it is possible in lattice simulations to compute observables relating to hadrons whose valence quarks have a different mass than the sea quarks, i.e. $m^{\text{val}} \neq m^{\text{sea}}$. This is illustrated in the diagram in Fig 5 for the case of a mesonic two-point function. It implies that one has more freedom to explore the dependence of physical observables on m^{val} and m^{sea} separately, and to compare the results to the predictions to Chiral Perturbation Theory [73] and its modified version for unequal sea and valence quark masses [81–83].

It is clear that the simulations listed in Table 1 do not have the correct value of n_f for kaon physics. In the absence of any sufficiently tested simulation algorithm capable of treating $n_f = 3$ flavours of dynamical fermions one is forced to introduce the strange quark as a valence quark by making the identifications

$$m_s = m^{\text{val}}, \quad m_{u,d} = m^{\text{sea}}, \quad m^{\text{val}} > m^{\text{sea}}. \quad (21)$$

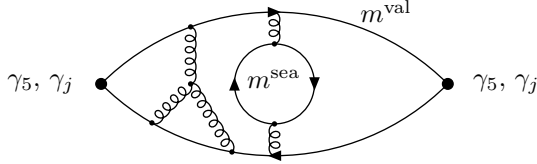


Figure 5. Quark and gluon contributions to the two-point function for a pseudoscalar (vector) meson in partially quenched QCD with $m^{\text{sea}} \neq m^{\text{val}}$.

This defines the so-called *partially quenched* approximation.

One should also bear in mind that the values of m^{sea} which are accessible in current simulations (especially for Wilson quarks) are still relatively large. This is easily seen by computing the ratio of the pseudoscalar to vector meson mass $m_{\text{PS}}/m_{\text{V}}$ (for $m^{\text{sea}} = m^{\text{val}}$) and comparing it to the physical ratio $m_{\pi}/m_{\rho} = 0.169$. For some of the simulations in Table 1 one finds [80, 84–87]

$$\frac{m_{\text{PS}}}{m_{\text{V}}} = \begin{cases} 0.69 - 0.83 & \text{SESAM} \\ 0.58 - 0.86 & \text{UKQCD} \\ 0.60 - 0.80 & \text{CP-PACS} \end{cases} \quad (22)$$

In order to make contact with the physical situation one has to study the dependence of observables on m^{sea} and extrapolate in m^{sea} to the physical value of m_{π}/m_{ρ} . Since the vector meson can decay into two pseudoscalars below $m_{\text{PS}}/m_{\text{V}} \approx 0.5$ such a naive extrapolation may, however, be misleading.

Several collaborations have investigated sea quark effects in the light hadron spectrum. CP-PACS [87] studied the continuum limit of hadron masses computed for $n_f = 2$ and compared it with the results of the quenched light hadron spectrum discussed before. Figure 6 shows the results for the masses of the K^* and ϕ mesons for $n_f = 0, 2$. This demonstrates clearly that the discrepancy with the experimentally observed spectrum is considerably reduced when sea quarks are “switched on”. The figure also illustrates that a reliable quantification of sea quark effects can only be made after the extrapolation to the continuum limit: at non-zero values of a the deviation between experiment and partially quenched QCD is enhanced, and thus one would come to the wrong conclusion about the size of dynamical quark effects.

Results for the vector-pseudoscalar mass splitting reported by UKQCD [85] also show that lattice data for this quantity approach the experimental value as the sea quark mass is decreased.

These findings are quite encouraging: they demonstrate that sea quarks have the expected

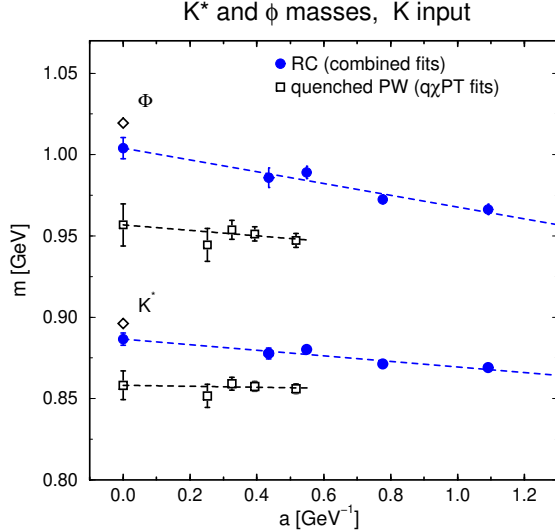


Figure 6. Scaling behaviour of vector mesons in quenched and partially quenched QCD [87].

effects on hadronic quantities. Of course, the remaining differences between partially quenched QCD and experiment seen in Fig. 6 have to be explained. It is reasonable to assume that the incorrect value of n_f for kaon physics will have some influence. Further studies are required in order to decide whether there is yet sufficient control over the extrapolations in m^{sea} , m^{val} , as well as the extrapolations to the continuum limit.

3.3. Sea quark effects in other observables

There are a number of observables which are particularly sensitive to sea quark effects. One example are flavour-singlet amplitudes which are relevant for quantities such as the η' mass. Unlike flavour non-singlet matrix elements these amplitudes receive contributions from disconnected diagrams and are thus sensitive to vacuum polarisation effects due to dynamical quarks and the value of n_f .

In a number of recent papers calculations of disconnected diagrams contributing to the η' mass [88, 89], the π -nucleon σ -term [90] and the flavour-singlet axial coupling of the proton [91] have been presented. Although some of the expected qualitative features of sea quark contributions to these observables have been seen [89], the main obstacles for more quantitative analyses are the high level of statistical noise encountered in the evaluation of disconnected diagrams and also the fact that $n_f = 3$ flavours cannot be simulated. It is estimated that the calculation of the disconnected contribution to the mass of

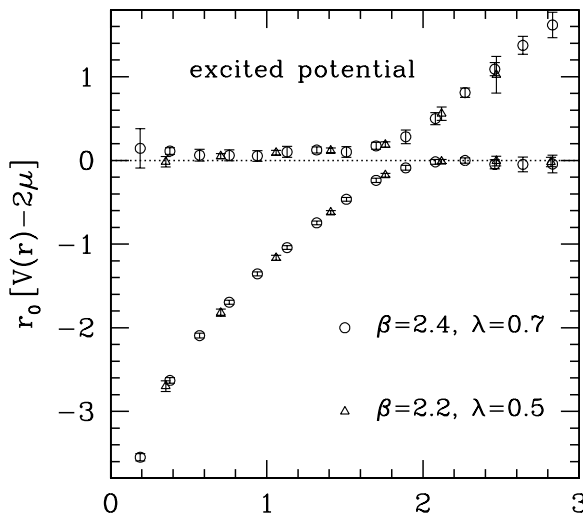


Figure 7. The static quark potential and the first excitation computed in the SU(2) Higgs model using a variational technique [100]. The flattening of the ground state for large separations indicates the breakdown of linear confinement.

flavour-singlet mesons is an order of magnitude more expensive than conventional correlators, so that more efficient numerical methods have to be developed and applied [92]. Therefore, there are no firm quantitative results for vacuum polarisation in flavour-singlet amplitudes at present. The current status of this field has been reviewed extensively in [93].

A phenomenon which is expected to occur in the presence of dynamical quarks is the breakdown of linear confinement, also called “string breaking”. This should manifest itself in a flattening-off of the static quark potential at a characteristic distance r_b at which the mass of two heavy-light mesons is energetically favoured over the energy of the flux tube which is responsible for the linearly rising potential between the static quarks. In QCD string breaking can be linked to decay rates of processes like $\Upsilon(4S) \rightarrow B\bar{B}$ [94] and is therefore of direct phenomenological relevance. Despite many recent efforts [80, 85, 95] there is no unambiguous sign for string breaking in simulations of QCD with $n_f = 2$ flavours of Wilson fermions, if the potential is determined by measuring Wilson loops. It has, however, been observed for QCD with staggered quarks [96, 97] and in QCD at finite temperature [98].

The reason for the failure to detect string breaking in QCD at zero temperature has been attributed to the bad projection properties of Wilson loops onto the state of the broken string.

This has been confirmed in studies in which the fermionic fields have been replaced by scalar fields (which are computationally much less demanding whilst preserving the underlying mechanism for string breaking to occur) [99–101]. In these studies string breaking was treated as a mixing phenomenon between the string and the two-“meson” state. This was achieved by supplementing the operator basis with operators having an explicit projection onto the broken string and by employing a variational approach to determine the energy levels. Indeed this more sophisticated method has provided clear evidence for string breaking (an example for the SU(2) Higgs model is shown in Fig. 7), and there are preliminary results [102, 103] which indicate that the approach is successful in QCD as well.

4. Light quark masses

Quark masses are fundamental parameters of the Standard Model, and their determination has been the subject of many recent activities. In particular, the mass of the strange quark, m_s , has received a lot of attention following the recent experimental results on ϵ'/ϵ [104]. Theoretical analyses of this quantity rely on m_s as one of the essential input parameters.

Ratios of the light quark masses are predicted by Chiral Perturbation Theory with a precision of a few percent [105]. In order to obtain individual quark masses it is thus sufficient to determine a particular linear combination using lattice QCD.

4.1. Non-perturbative renormalisation

A convenient starting point to discuss lattice calculations of light quark masses is the PCAC relation. For charged kaons it can be written as

$$f_K m_K^2 = (\bar{m}_u + \bar{m}_s) \langle 0 | \bar{u} \gamma_5 s | K \rangle. \quad (23)$$

In order to determine the sum of quark masses $(\bar{m}_u + \bar{m}_s)$ using the experimental result for $f_K m_K^2$, it suffices to compute the matrix element $\langle 0 | \bar{u} \gamma_5 s | K \rangle$ in a lattice simulation. The renormalisation of the pseudoscalar density $\bar{u} \gamma_5 s$ is, however, scale- and scheme-dependent. By convention quark masses are quoted in the $\overline{\text{MS}}$ scheme of dimensional regularisation at some reference scale μ . Therefore the relation between the pseudoscalar densities in the $\overline{\text{MS}}$ scheme and lattice regularisation must be computed, viz

$$(\bar{u} \gamma_5 s)_{\overline{\text{MS}}} = Z_P(g_0, a\mu) (\bar{u} \gamma_5 s)_{\text{lat}}. \quad (24)$$

Here g_0 is the bare coupling, and μ is the subtraction point in the $\overline{\text{MS}}$ scheme. The renormalisation

factor Z_P has been computed in lattice perturbation theory for several discretisations. However, the limitations of lattice perturbation theory are well known, and in order to remove all doubts about the reliability of the matching procedure it is evident that a non-perturbative determination of the renormalisation factor is required.

One of the main obstacles for a fully non-perturbative matching procedure are the large scale differences between the low-energy regime, which is the domain of the lattice regularisation scheme and the high-energy, perturbative regime where the $\overline{\text{MS}}$ scheme is defined. This technical difficulty can be overcome by introducing an intermediate scheme X, as shown schematically in Fig. 8. The problem is thus split into two parts. The first is the matching of the bare current quark mass $m_{\text{lat}}(a)$ to the running mass in the intermediate scheme, $\overline{m}_X(\mu)$. This amounts to computing $Z_P(g_0, a\mu_0)$ between the lattice scheme and scheme X for a range of bare couplings g_0 at a fixed scale μ_0 . The second part is the determination of the scale dependence of the running mass $\overline{m}_X(\mu)$ from μ_0 up to very high energies, where the perturbative relation between \overline{m}_X and $\overline{m}_{\overline{\text{MS}}}$ can be expected to be reliable. Through this two-step process the use of lattice perturbation theory is completely avoided.

So far two proposals to define a suitable intermediate scheme have been put forward. The first has been introduced in ref. [106] and imposes non-perturbative renormalisation conditions on Green functions of local operators, computed between off-shell quark and gluon states, with virtualities μ , in a fixed gauge. In the case of the pseudoscalar density such a normalisation condition reads

$$Z_P(g_0, a\mu) Z_q^{-1}(g_0, a\mu) \Gamma_P(ap) \Big|_{p^2=\mu^2} = 1. \quad (25)$$

Here Γ_P denotes the amputated Green function of $\bar{q}\gamma_5 q$, and Z_q is the quark wavefunction renormalisation factor (which is easily computed in a lattice simulation). Typically this relation is evaluated in the Landau gauge. This choice of intermediate scheme is referred to as the Regularisation Independent (RI) scheme, in which the rôle of the renormalisation scale is played by the virtuality μ of the quark states. The scale dependence can then be probed by choosing different external momenta for the quark fields used to compute Γ_P . Provided that the virtualities can be fixed such that

$$\Lambda_{\text{QCD}} \ll \mu \ll a^{-1} \quad (26)$$

the perturbative matching between the RI and $\overline{\text{MS}}$ schemes expected to work well.

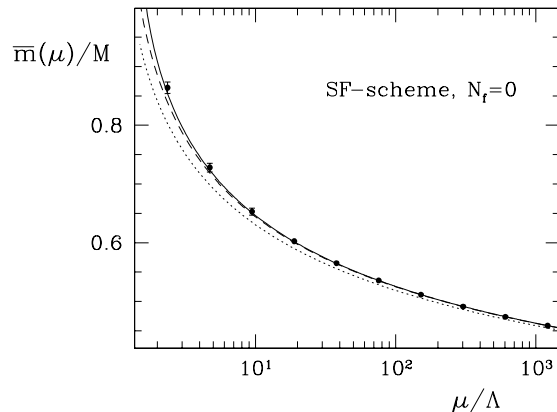


Figure 9. Non-perturbative scale evolution of $\overline{m}_{\text{SF}}/M$ computed in lattice simulations of the SF (solid circles). The dotted, dashed and solid lines correspond to the scale evolution computed using the 2/1-, 2/2 and 3/2-loop expressions for the RG β -function and the anomalous dimension.

Another intermediate scheme is defined using the Schrödinger Functional (SF) of QCD [107–109]. This scheme is based on the formulation of QCD in a finite volume of size $L^3 \cdot T$ with inhomogeneous (Dirichlet) boundary conditions in the time direction. Non-perturbative renormalisation conditions can then be imposed at scale $\mu = 1/L$ and zero quark mass. An attractive feature of the SF scheme is that it allows to compute the scale dependence non-perturbatively over several orders of magnitude, using a recursive finite-size scaling technique. Thus, once the scale dependence of \overline{m}_{SF} is known up to energies of around 100 GeV one can continue the scale evolution to infinite energy using the perturbative renormalisation group functions and thereby extract the renormalisation group invariant (RGI) quark mass M . In Fig. 9 the scale dependence of $\overline{m}_{\text{SF}}/M$ computed in quenched QCD [110] is shown and compared to the perturbative scale evolution.

The left-most point in Fig. 9 corresponds to a scale $\mu_0 \sim 275$ MeV. Here one reads off [110]

$$\frac{M}{\overline{m}_{\text{SF}}} = 1.157 \pm 0.015. \quad (27)$$

The matching between lattice regularisation and $\overline{\text{MS}}$ scheme via the SF is completed by computing the renormalisation factor $Z_P(g_0, a\mu_0)$ for a particular fermion discretisation, at fixed $\mu_0 = 275$ MeV, for a range of bare couplings. In ref. [110] this has been performed for the $O(a)$ improved Wilson action, for couplings which correspond to lattice spacings in the range

$$a \sim 0.1 - 0.045 \text{ fm.} \quad (28)$$

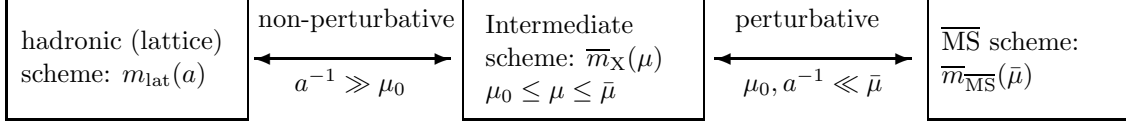


Figure 8. Schematic relation between quark masses in lattice regularisation and the $\overline{\text{MS}}$ scheme through an intermediate renormalisation scheme X.

4.2. Light quark masses in quenched QCD

Estimates for the light quark masses for several fermion lattice actions and using non-perturbative renormalisation (implemented either in the RI or SF schemes) have been reported recently [50, 111–113]. As an illustration I shall describe in some detail the determination of the strange quark mass along the lines of ref. [112], in which the non-perturbative renormalisation factors computed in ref. [110] were used.

The average light quark mass m_l is defined as

$$m_l = \frac{1}{2}(m_u + m_d). \quad (29)$$

By combining the result for $M/\overline{m}_{\text{SF}}$ from eq. (27) with the factor $Z_P(g_0, a\mu_0)$ and the PCAC relation eq. (23) one obtains an expression for the sum of RGI quark masses $(M_s + M_l)$ in units of the kaon decay constant

$$\frac{M_s + M_l}{f_K} = \frac{M}{\overline{m}_{\text{SF}}} \frac{m_K^2}{Z_P(g_0, a\mu_0) G_K(a)} + O(a^2). \quad (30)$$

Here, up to a small mass dependent factor which arises in the $O(a)$ improved Wilson theory, G_K is equal to the matrix element of the pseudoscalar density evaluated at the kaon mass. At this point all reference to the intermediate SF scheme is cancelled in the product $M/(\overline{m}_{\text{SF}} Z_P)$. What remains to be specified is the experimental value of m_K^2 expressed in units of some quantity which sets the lattice scale (e.g. the hadronic radius r_0 [115, 116]). The results for $(M_s + M_l)/f_K$ as obtained from eq. (30) can now be extrapolated to the continuum limit. This is shown in Fig. 10, which also illustrates that the remaining discretisation errors in the $O(a)$ improved theory are consistent with a leading behaviour proportional to a^2 .

Using the experimental value $f_K = 160 \pm 2 \text{ MeV}$ one obtains in the continuum limit

$$M_s + M_l = 140 \pm 5 \text{ MeV}. \quad (31)$$

This result can now be converted into $\overline{m}_s^{\overline{\text{MS}}}(\mu)$ at $\mu = 2 \text{ GeV}$. First one combines eq. (31) with the prediction from Chiral Perturbation Theory [105]

$$M_s/M_l = 24.4 \pm 1.5. \quad (32)$$

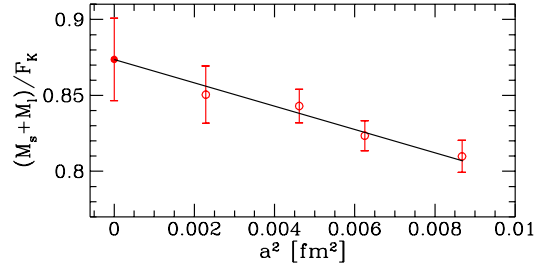


Figure 10. Continuum extrapolation of $(M_s + M_l)/f_K$. The lattice scale is set by hadronic radius r_0 .

By integrating the (4-loop) perturbative RG functions in the $\overline{\text{MS}}$ scheme one obtains

$$\overline{m}^{\overline{\text{MS}}}(\mu)/M = 0.7208 \text{ at } \mu = 2 \text{ GeV}. \quad (33)$$

Finally, combining eqs. (31), (32) and (33) yields the final result in the quenched approximation [112]

$$\overline{m}_s^{\overline{\text{MS}}}(2 \text{ GeV}) = 97 \pm 4 \text{ MeV}. \quad (34)$$

The quoted uncertainty of $\pm 4 \text{ MeV}$ contains all errors, except those due to quenching. As mentioned in the introduction, the conversion into physical units is ambiguous in the quenched approximation. For $\overline{m}_s^{\overline{\text{MS}}}(2 \text{ GeV})$ the resulting uncertainty was estimated to amount to $\sim 10\%$.

A compilation of recent results for m_s and m_l in quenched QCD is shown in Table 2. When comparing the results one has to bear in mind that systematic errors – where shown – have not been estimated in a uniform manner, or have sometimes been combined in quadrature with the statistical errors. Also, the conversion into physical units has been performed using different quantities. Nevertheless, the picture that emerges is quite encouraging. Estimates for the strange quark mass in quenched QCD cluster around 100 MeV and around 4.5 MeV for the average up and down quark mass. Different discretisations such as Wilson, staggered and Domain Wall fermions as well as different implementations of non-perturbative quark mass renormalisation yield broadly consistent results.

Table 2. Estimates for the quark masses m_s and m_l in the $\overline{\text{MS}}$ scheme at $\mu = 2 \text{ GeV}$ in quenched QCD. Also shown is the choice of intermediate renormalisation scheme X and the lattice Dirac operator. Crosses indicate that non-perturbative renormalisation and/or a continuum extrapolation has not been implemented.

Collab.	m_l	m_s	X	S_F	$a \rightarrow 0$
BGLM [117]	4.5(5)	111(9)	RI	D_{SW}	\times
QCDSF [113]	4.4(2)	105(4)	SF	D_{SW}	\checkmark
RBC [114]		130(11)(18)	RI	D^{DWF}	\times
ALPHA/UKQCD [112]		97(4)	SF	D_{SW}	\checkmark
CP-PACS [71]	4.55(18)	115(2)	\times	D_W	\checkmark
BSW [49]		96(26)	\times	D^{DWF}	\checkmark
JLQCD [111]	4.23(29)	106(7)	RI	D_{stag}	\checkmark
Becirevic et al. [118]	4.5(4)	111(12)	RI	D_{SW}	\times

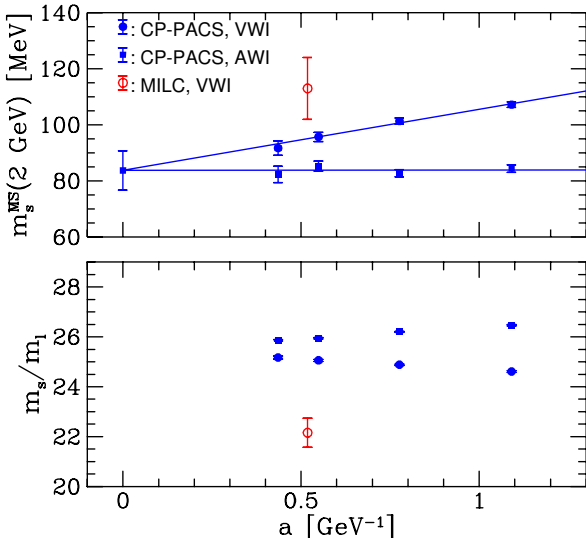


Figure 11. The strange quark mass and the ratio m_s/m_l extracted using either the vector or axial vector Ward identities plotted versus the lattice spacing.

4.3. Sea quark effects in m_s and m_l

An important issue, especially for phenomenological applications of lattice calculations of the light quark masses is the influence of dynamical quarks. Estimates for m_l and m_s computed in partially quenched QCD have been reported in [84, 87, 119, 120]. Since non-perturbative renormalisation has so far not been applied for $n_f = 2$, all of these calculations rely on perturbation theory to match the quark masses in the lattice and $\overline{\text{MS}}$ schemes.

The most comprehensive study so far has been presented by CP-PACS [87] in which not only the m^{sea} -dependence has been investigated but also

the extrapolation to the continuum limit. The scaling behaviour of $\overline{m}_s^{\overline{\text{MS}}}(2 \text{ GeV})$ extracted either from the vector or axial vector Ward identities (labelled VWI or AWI respectively) is shown in the upper part of Fig. 11. In spite of the large differences observed for the two methods at non-zero lattice spacing, the results are consistent with a common continuum limit, where $\overline{m}_s^{\overline{\text{MS}}}(2 \text{ GeV}) = 84 \pm 7 \text{ MeV}$. This is significantly lower than the quenched results discussed earlier. However, many systematic effects are not as well controlled as in the quenched case, so that further studies, employing non-perturbative renormalisation and investigating the n_f -dependence are required before a substantial decrease of quark masses relative to the quenched results can be confirmed. It is interesting, though, that the ratio m_s/m_l , in which many systematic effects are expected to cancel, extrapolates to $m_s/m_l = 26 \pm 3$ (c.f. lower part of Fig. 11). This value is in excellent agreement with the prediction from Chiral Perturbation Theory, eq. (32). The preliminary results by the MILC Collaboration [120], which are also shown in the figure, have been computed at a fixed value of m^{sea} corresponding to $m_\pi/m_\rho = 0.56$. This may explain why they are different from the CP-PACS results, which in turn have been extrapolated in m^{sea} to the physical value.

For phenomenological applications one may be tempted to convert the results presented here into a global estimate. Before more thorough studies of dynamical quark effects become available, I consider the quenched results (e.g. eq. (34)) the most reliable estimate. By accounting for the systematic errors due to using the quenched approximation one can then quote a global result for m_s as

$$\overline{m}_s^{\overline{\text{MS}}}(2 \text{ GeV}) = 100 \pm 5 \text{ (stat)} {}^{+10}_{-20} \text{ (syst)} \text{ MeV.} \quad (35)$$

The systematic error in the above estimate incorporates the afore-mentioned scale ambiguity of 10 MeV, as well as the observed decrease in the central value for $n_f = 2$ dynamical flavours.

5. Glueballs and heavy hybrids

Historically glueball masses were among the first quantities to be computed in lattice gauge theories. Over the years the calculations have become more refined, for instance, by constructing efficient glueball operators, by studying the approach to the continuum limit, and by including higher spin states.

The main difficulty in glueball calculations is the relatively high level of statistical noise in the correlation functions from which the masses are extracted. Here I shall focus on recent calculations in which this problem has been alleviated by using anisotropic lattice actions. Hence, from now on I shall distinguish between spatial and temporal lattice spacings, a_s and a_t , respectively. If $C_G(t)$ denotes the correlation function of a glueball operator $G(x)$, then its asymptotic behaviour for large separations t is given by

$$C_G(t) = \sum_{\vec{x}} \langle G(\vec{x}, t) G^\dagger(0) \rangle \sim e^{-(a_t M_G)(t/a_t)}. \quad (36)$$

That is, the exponential decay of $C_G(t)$ is governed by the glueball mass in units of the temporal lattice spacing. Therefore, the larger $a_t M_G$, the quicker the decay of $C_G(t)$, so that its asymptotic behaviour may be difficult to isolate before the statistical noise becomes too large. By introducing an anisotropic lattice action with $a_t \ll a_s$, one can simultaneously achieve slow exponential fall-off of $C_G(t)$ whilst preserving large spatial volumes in physical units. The spatial volume in *lattice units*, however, can be kept small if a_s is large in physical units, so that the calculations are more manageable. Typical values of a_s are

$$a_s \approx 0.2 - 0.4 \text{ fm}, \quad (37)$$

while the “aspect ratio” $\xi \equiv a_s/a_t$ is usually taken in the range

$$\xi = 3 - 5. \quad (38)$$

The idea of using anisotropic lattices in glueball calculations is not new: it was used already 16 years ago [121], before the advent of “smearing” techniques to construct glueball operators for which the asymptotic behaviour in the correlation function sets in very quickly.

The idea of anisotropic lattice actions has been revived by the desire to compute the higher glueball states more accurately and to use very coarse spatial

lattices so that these calculations can be performed on smaller computers. However, by pushing to very large values of a_s one may suffer from uncontrollably large discretisation effects. Here, the Symanzik improvement programme can be used to eliminate the leading lattice artefacts, so that the extrapolation of results obtained on coarse, anisotropic lattices is sufficiently controlled.

In the rest of this section I shall mainly discuss recent results for the spectra of glueballs and heavy hybrids obtained using anisotropic actions. For more comprehensive reviews I refer the reader to refs. [122, 123].

5.1. Glueball spectrum in quenched QCD

In two recent papers Morningstar and Peardon [124] have presented results for the quenched glueball spectrum below 4 GeV computed using an anisotropic, $O(a_s^2)$ improved gluon lattice action with aspect ratios $\xi = 3$ and 5. Thus, improvement has been employed to reduce artefacts associated with the spatial lattice spacing only. Non-perturbative determinations of the relevant improvement coefficients are not available for the case at hand, so that one relies on their estimates in mean-field improved perturbation theory. This procedure does not completely remove lattice artefacts of order a_s^2 . One thus expects leading cutoff effects of order

$$g^2 a_s^2, a_s^4, a_t^2. \quad (39)$$

Since the lattice breaks rotational symmetry, glueball operators are, as usual, constructed from representations of the octahedral group: A_1, A_2, E, T_1, T_2 . Figure 12 shows the scaling behaviour of the glueball masses in the $PC = ++$ channel, extracted from the various representations. The plot nicely demonstrates the restoration of rotational symmetry in the limit $a_s \rightarrow 0$. For instance, both the E and T_2 representations describe the spin-2 glueball in the continuum limit, but differ significantly at large, non-zero lattice spacings.

The observed curvature in the continuum extrapolation of the scalar (0^{++} and 0^{*++}) glueballs suggests that both $O(a_s^2)$ and $O(a_s^4)$ lattice artefacts are sizeable for these states. Hence, if lattice spacings as large as $a_s \approx 0.4$ fm are included one has to use a more complicated model function for the continuum extrapolation, which ultimately leads to a loss of statistical precision for these states.

The final, continuum results for glueball states from ref. [124] for a number of different J^{PC} assignments are shown in Fig. 13, in units of the hadronic radius r_0 and in physical units on the left and right margins, respectively.

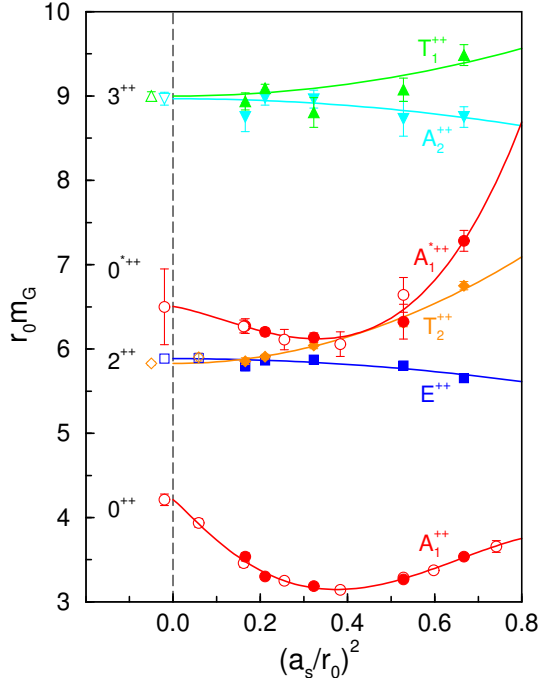


Figure 12. Continuum extrapolations of glueballs computed for different representations of the octahedral group on anisotropic lattices [124] for $PC = ++$.

The masses of the two lowest-lying glueballs obtained on anisotropic lattices can now be compared to results using more conventional techniques. A meaningful comparison can be made by expressing results from different simulations in units of a common scale, for which I have again chosen the hadronic radius r_0 . Thus, the results from refs. [122, 125, 126] have been expressed or converted in units of r_0 , and whenever necessary the continuum extrapolation has been re-done. The resulting masses for the lowest scalar and tensor glueballs are listed in Table 3 together with the value of the aspect ratio ξ and the year in which the calculation was carried out. It is also indicated whether a continuum extrapolation has been performed.

The table shows that the results obtained in different simulations are in broad agreement. If those estimates are to be used for phenomenological purposes, it should be kept in mind that they are valid in the quenched approximation. This implies that the conversion into physical units (e.g. by using $r_0 = 0.5$ fm) is ambiguous. Also, the influence of dynamical quark effects, and, perhaps most importantly, the issue of glueball-meson mixing has not been addressed for the results presented in Table 3. The latter has been studied, e.g. in ref. [127–129], and very recently in ref. [130], which

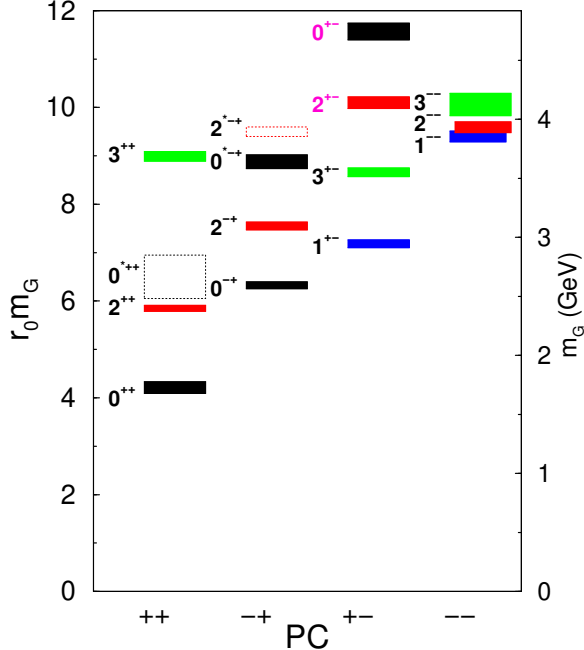


Figure 13. Results for the quenched glueball spectrum in the continuum limit from ref. [124].

also contains a detailed calculation of the spectrum of light quarkonia in quenched QCD. Overall, it is found that physical glueball masses are quite sensitive to the details of the proposed mixing pattern.

Dynamical quark effects in the glueball spectrum have been studied in [131] and [92]. Whereas ref. [131] reports no significant deviation of glueball masses computed for $n_f = 2$ (within large errors), results by UKQCD [92] indicate much lower estimates in unquenched simulations for both the scalar glueball and quarkonium state. However, a number of effects, e.g. the question of lattice artefacts have to be addressed in much more detail before these results can be confirmed.

5.2. Heavy quarkonia and hybrids

In addition to glueballs the spectrum of quarkonia and hybrids can also be calculated in lattice QCD. Such calculations may provide hints especially for the heavy quark sector, where very little experimental data exists for hybrid states. Thus, on the lattice one would like to compute the masses of states which are obtained from quark bilinears by inserting one or more gluons, such as $\bar{b}gb$ and $\bar{c}gc$.

Ideally a fully relativistic treatment of the heavy quarks would be desirable. However, for the currently accessible range of lattice spacings, for

Table 3. Comparison of the two lowest glueball masses in units of r_0 .

Collab.	$r_0 m_{0++}$	$r_0 m_{2++}$	ξ	$a \rightarrow 0$	year
M+P [124]	4.21(11)(4)	5.85(2)(6)	3, 5	✓	1999
GF11 [126]	4.33(10)	6.04(18)	1	✓	1999
Teper [122]	4.35(11)	6.18(21)	1	✓	1998
UKQCD [125]	4.05(16)	5.84(18)	1	✗	1993

which $a \gtrsim 0.05$ fm (corresponding to $a^{-1} \lesssim 4$ GeV) one expects large lattice artefacts in the charm sector, while the b quark with a mass above 4 GeV cannot at all be simulated directly. If anisotropic lattices with coarse spatial lattice spacings of $a_s = 0.2 - 0.4$ fm are employed, the situation is even worse.

One way to address the problem of large cutoff effects in the heavy quark sector is to resort to an effective, non-relativistic treatment [132], by introducing a cutoff Λ such that

$$\Lambda \sim a^{-1} < m_Q, \quad (40)$$

where m_Q is the mass of the heavy quark. In other words, relativistic states above Λ are excluded. Based on this approximation one can write down a discretised, effective, non-relativistic QCD action (NRQCD). On a formal level this approximation of QCD can be viewed as an expansion in the strong coupling constant and the 4-velocity v of the heavy quark. In this formulation the lattice spacing acts both as the UV regulator and the non-relativistic cutoff. This implies in turn that the continuum limit $a \rightarrow 0$ cannot be taken, since otherwise the non-relativistic approximation breaks down. Therefore, in order for cutoff effects to be under control one relies on a “window” in a where NRQCD works well and lattice artefacts are small at the same time.

Two groups have recently reported results for heavy quarkonia and hybrids using NRQCD on anisotropic lattices [133, 134]. Both have used the $O(a_s^2)$ mean-field improved gluon action for $\xi = 3, 5$ and an NRQCD action expanded in the 4-velocity to order $m_Q v^2$. At this order, spin interactions are neglected. Therefore one expects spin degeneracies for the S - and P -wave quarkonium states, as well as for each of the hybrid states H_1 , H_2 and H_3 with quantum numbers $J^{PC} = 1^{--}$ (H_1), 1^{++} (H_2) and 0^{++} (H_3), respectively.

A convenient way to present the results is to quote the hybrid- S -wave splittings $\delta(H_i - S)$, $i = 1, 2, 3$. In Fig. 14 those splittings, normalised to the $1S - 1P$ quarkonium splitting, are plotted versus

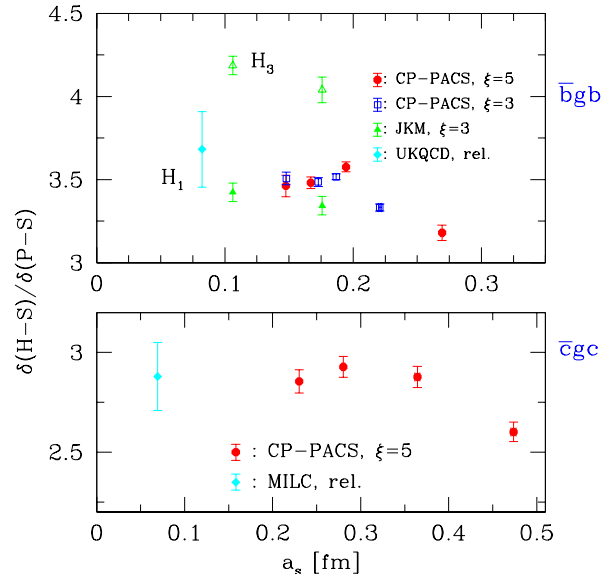


Figure 14. The hybrid splittings in the charm and bottom sectors from NRQCD on anisotropic lattices. Diamonds denote the results using relativistic heavy quarks.

the spatial lattice spacing a_s . Focussing on the upper part of the figure which shows the spectrum in the bottomonium sector, one sees that anisotropy effects appear to be under control: the results by CP-PACS [133] obtained for $\xi = 3, 5$ are consistent within errors. Furthermore, the data from both groups support the existence of a window for $a_s \approx 0.1 - 0.2$ fm, where discretisation effects are small: in that range the variation of the results with a_s is roughly as large as the statistical precision. It is obvious, though, that this is no longer the case for $a_s > 0.2$ fm. Similar observations apply in the charmonium sector shown in the lower part of Fig. 14, where the scaling window appears to be somewhat larger.

The results for the lowest $\bar{b}gb$ hybrid splitting

obtained on anisotropic lattices are [133, 134]

$$\delta(H_1 - S) = \begin{cases} 1.542(8) \text{ GeV} & \text{CP-PACS} \\ 1.49(2)(5) \text{ GeV} & \text{KJM} \end{cases} \quad (41)$$

For both charmonium and bottomonium hybrids the results can be compared to those in which the heavy quarks were treated relativistically, involving extrapolations in the heavy quark mass [135, 136]. These data points are included as diamonds in Fig. 14 and are consistent with those using anisotropic actions. This nicely illustrates how complementary formulations of heavy quarks can be used to control different systematic effects.

6. Other topics

The topics which are presented in this section could not be reviewed extensively, but nevertheless I shall briefly summarise the current status and refer the interested reader to the recent literature.

6.1. Kaon weak matrix elements

Lattice calculations for the B -parameter B_K , which is relevant for $K^0 - \bar{K}^0$ mixing, as well as matrix elements for $K \rightarrow \pi\pi$ and ϵ'/ϵ have recently been reviewed by Kuramashi [137] and Martinelli [138].

There are now many calculations of B_K using different discretisations of the Dirac operator. For staggered fermions the most recent result quoted in the naive dimensional reduction (NDR) scheme is

$$B_K^{\text{NDR}}(2 \text{ GeV}) = 0.628 \pm 0.048. \quad (42)$$

Further improvements of this result could be achieved through the implementation of non-perturbative renormalisation. Simulations using Wilson fermions [139] are consistent with the result in eq. (42). Estimates for B_K using Domain Wall fermions have also been presented [46, 47].

Compared to $K^0 - \bar{K}^0$ mixing the lattice predictions for matrix elements relevant for $K \rightarrow \pi\pi$ and ϵ'/ϵ are a lot less accurate, and a number of systematic effects have to be better controlled. Details can be found in [137, 138]. A surprising, *negative* result for $\text{Re}(\epsilon'/\epsilon)$ has been reported recently in [48]. However, given that it has been obtained using the relatively new technology of Domain Wall fermions, future studies are required to clarify this issue.

6.2. B decay matrix elements

Decays of heavy-light mesons have long been studied in lattice gauge theories. The current status

has been reviewed by Hashimoto [140]. Semi-leptonic heavy-to-light and heavy-to-heavy decays have been analysed in the quenched approximation for several formulations of heavy quarks. Lattice estimates for heavy-light decay constants such as f_B have stabilised in the quenched approximation, and their current values can be summarised as [140]

$$f_B = 170 \pm 20 \text{ MeV}, \quad f_{B_s}/f_B = 1.15 \pm 0.04. \quad (43)$$

Present activities center on the quantification of sea quark effects. Preliminary estimates suggest that heavy-light decay constants increase by up to 20% for $n_f = 2$ flavours of dynamical quarks at non-zero values of the lattice spacing [141]. However, a detailed scaling analysis is still required in order to separate sea quark effects from lattice artefacts, so that the large increase in f_B for $n_f = 2$ does, in my view, not constitute a solid result at present.

6.3. Structure functions

This topic has recently received a lot of attention and has been reviewed by Petronzio [142]. Current activities include the implementation of non-perturbative renormalisation of parton density operators, using either the RI or SF schemes described in section 4. The SF scheme has been employed to determine non-perturbatively the scale dependence of the twist-two, non-singlet parton density operator [143]. Other projects in this area include calculations of higher twist contributions to the pion structure function [144].

7. Summary

The most significant theoretical development in Lattice Gauge Theory has surely been the progress made in formulating chiral symmetry at non-zero lattice spacing. It is now clear that chiral gauge theories can be put on the lattice in a consistent way, without breaking the gauge symmetry. This shows that a regularisation of the Standard Model exists beyond perturbation theory.

Lattice simulations of QCD are becoming ever more refined, thanks to a number of technical developments, such as the implementation of the Symanzik improvement programme, non-perturbative renormalisation, the use of anisotropic lattices and bigger, more efficient simulations with dynamical quarks.

The quenched approximation, which is still widely used, works surprisingly well. This is good news for many computationally more demanding applications, for which the quenched approximation will be useful for some time in the future. There

are now many attempts to quantify the effects of dynamical quarks, and in some cases they have been found to be significant. This has only been possible after all other systematic effects, including lattice artefacts, could be controlled at the level of a few percent.

Although lattice QCD may not yet be the ultimate phenomenological tool, it is clear that enormous progress towards this goal has been, and will be made.

Acknowledgements

I am grateful to Arifa Ali Khan, Oliver Bär, Claude Bernard, Ruedi Burkhalter, Chris Dawson, Takashi Kaneko, Thomas Manke, Colin Morningstar, Petrus Pennanen, Gerrit Schierholz, Hugh Shanahan, Amarjit Soni and Matt Wingate for making their results available to me. I thank Sinya Aoki, Ruedi Burkhalter, Michael Haas, Shoji Hashimoto, Kazuyuki Kanaya and Frithjof Karsch for useful discussions, and Karl Jansen for a critical reading of the manuscript. I am grateful to Akira Ukawa for the kind hospitality at the Center for Computational Physics, University of Tsukuba, where most of this talk was prepared. The support by PPARC through the award of an Advanced Fellowship is gratefully acknowledged.

References

- [1] Wilson K G 1974 *Phys. Rev.* **D10** 2445
- [2] Laermann E 1998 *Nucl. Phys. B (Proc. Suppl.)* **63** 114
- [3] Alford M 1999 *Nucl. Phys. B (Proc. Suppl.)* **73** 161
- [4] Karsch F 1999, plenary talk presented at *Lattice '99*, hep-lat/9909006
- [5] Smit J 1998 *Nucl. Phys. B (Proc. Suppl.)* **63** 89
- [6] Laine M and Rummukainen K 1999 *Nucl. Phys. B (Proc. Suppl.)* **73** 180
- [7] Fodor Z 1999, plenary talk presented at *Lattice '99*, hep-lat/9909162
- [8] Negele J 1999 *Nucl. Phys. B (Proc. Suppl.)* **73** 92
- [9] Teper M 1999, plenary talk presented at *Lattice '99*, hep-lat/9909124
- [10] Bowick M 1998 *Nucl. Phys. B (Proc. Suppl.)* **63** 77
- [11] Thorleifsson G *Nucl. Phys. B (Proc. Suppl.)* **73** 133
- [12] Lüscher M, in Hamburg 1997, Lepton photon interactions, p. 185, hep-ph/9711205
- [13] Sharpe S, in Vancouver 1998, High energy physics, p. 171, hep-lat/9811006
- [14] Nielsen H B and Ninomiya M 1981, *Phys. Lett.* **B105** 219; *Nucl. Phys.* **B185** 20; *Nucl. Phys.* **B193** 173
- [15] Kogut J and Susskind L 1975 *Phys. Rev. D* **11** 395
- [16] Symanzik K 1982, in: Mathematical problems in theoretical physics, eds. R. Schrader et al., Lecture Notes in Physics, Vol. 153 (Springer, New York);
- [17] Symanzik K 1983 *Nucl. Phys.* **B226** 187 and 205
- [18] Hasenfratz P and Niedermayer F 1994 *Nucl. Phys.* **B414** 785; Hasenfratz P 1998 *Nucl. Phys. B (Proc. Suppl.)* **63** 53; *Nucl. Phys. B* **525** 401
- [19] Sheikholeslami B and Wohlert R 1985 *Nucl. Phys.* **B259** 572
- [20] Lüscher M, Sint S, Sommer R and Weisz P 1996 *Nucl. Phys.* **B478** 365
- [21] Lüscher M, Sint S, Sommer R, Weisz P and Wolff U 1997 *Nucl. Phys.* **B491** 323
- [22] Edwards R G, Heller U M and Klassen T R 1998 *Phys. Rev. Lett.* **80** 3448
- [23] Jansen K and Sommer R 1998 *Nucl. Phys. B* **530** 185
- [24] Lüscher M, Sint S, Sommer R and Wittig H 1997 *Nucl. Phys.* **B491** 344
- [25] Bhattacharya T et al. 1999, hep-lat/9904011, hep-lat/9909092 and hep-lat/9909115
- [26] Wittig H 1998 *Nucl. Phys. B (Proc. Suppl.)* **63** 47
- [27] Heitger J (ALPHA Collaboration) 1999 *Nucl. Phys.* **B557** 309
- [28] Alford M, Klassen T R and Lepage G P 1997 *Nucl. Phys.* **B496** 377; 1998 *Phys. Rev. D* **58** 034503
- [29] Lepage G P and Mackenzie P B 1993 *Phys. Rev.* **D48** 2250
- [30] Klassen T R 1999 *Nucl. Phys. B (Proc. Suppl.)* **73** 918
- [31] DeGrand T, Hasenfratz A and Kovács T 1999 *Nucl. Phys.* **B547** 259
- [32] Albanese M et al. 1987 *Phys. Lett.* **192B** 163
- [33] DeGrand T 1999 *Phys. Rev. D* **60** 094501
- [34] Stephenson M, DeTar C, DeGrand T and Hasenfratz A 1999, hep-lat/9910023
- [35] Ginsparg P and Wilson K G 1982 *Phys. Rev. D* **25** 2649
- [36] Kaplan D B 1992 *Phys. Lett.* **B288** 342
- [37] Narayanan R and Neuberger H 1993 *Phys. Lett.* **B302** 62; 1994 *Nucl. Phys.* **B412** 574;
- [38] Narayanan R and Neuberger H 1995 *Nucl. Phys.* **B443** 305
- [39] Shamir Y 1993 *Nucl. Phys.* **B406** 90; Shamir Y and Furman V 1994 *Nucl. Phys.* **B439** 54

[40] Blum T 1999 *Nucl. Phys. B (Proc. Suppl.)* **73** 167

[41] Neuberger H 1999, hep-lat/9909042

[42] Lüscher M 1999, hep-lat/9909150

[43] Wu L 1999, hep-lat/9909117

[44] Fleming G 1999, hep-lat/9909140

[45] Vranas P et al. 1999 *Nucl. Phys. B (Proc. Suppl.)* **73** 456

[46] Blum T and Soni A 1997 *Phys. Rev. Lett.* **79** 3595

[47] Blum T and Soni A 1999, hep-lat/9909108; Soni A, these proceedings.

[48] RIKEN/BNL/CU Collaboration (Blum T et al.) 1999, hep-lat/9908025

[49] Blum T, Soni A and Wingate M 1999 *Phys. Rev.* **D60** 114507

[50] Wingate M (RIKEN/BNL/CU Collaboration) 1999, hep-lat/9909101

[51] Hasenfratz P, Laliena V and Niedermayer F 1998 *Phys. Lett.* **B427** 125

[52] Lüscher M 1998 *Phys. Lett.* **B428** 342

[53] Lüscher M 1999 *Nucl. Phys.* **B549** 295

[54] Lüscher M 1999, hep-lat/9904009

[55] Frolov S A and Slavnov A A 1993 *Phys. Lett.* **B309** 344

[56] Neuberger H 1998 *Phys. Lett.* **B417** 414

[57] Neuberger H 1998 *Phys. Lett.* **B427** 453

[58] Narayanan R 1998 *Phys. Rev.* **D58** 097501

[59] Witten E 1982 *Phys. Lett.* **B117** 324

[60] Neuberger H 1998 *Phys. Lett.* **B437** 117

[61] Bár O and Campos I 1999, hep-lat/9909081

[62] Edwards R G, Heller U M and Narayanan R 1999 *Phys. Rev.* **D59** 094510

[63] Damgaard P H, Edwards R G, Heller U M and Narayanan R 1999, hep-lat/9907016

[64] Hernández P, Jansen K and Lellouch L 1999, hep-lat/9907022

[65] Hernández P, Jansen K and Lüscher M 1999 *Nucl. Phys.* **B552** 363

[66] Edwards R G, Heller U M and Narayanan R 1999 *Nucl. Phys.* **B540** 457

[67] Kennedy A D, Horváth I and Sint S 1999 *Nucl. Phys. B (Proc. Suppl.)* **73** 834

[68] Boriçi A 1999 *Phys. Lett.* **B453** 46

[69] UKQCD Collaboration (McNeile C et al.) 1999, hep-lat/9909059

[70] DeGrand T 1999, hep-lat/9908037

[71] CP-PACS Collaboration (Aoki S et al.) 1999, hep-lat/9904012

[72] Butler F et al. 1994 *Nucl. Phys.* **B430** 179

[73] Gasser J and Leutwyler H 1985 *Nucl. Phys.* **B250** 465

[74] Bernard C W and Golterman M F L 1992 *Phys. Rev.* **D46** 853

[75] Sharpe S R 1992 *Phys. Rev.* **D46** 3146

[76] MILC Collaboration (Bernard C et al.) 1998 *Phys. Rev. Lett.* **81** 3087

[77] UKQCD Collaboration (Bowler K C et al.) 1999, hep-lat/9910022

[78] Lüscher M and Weisz P 1985 *Commun. Math. Phys.* **97** 59; *Phys. Lett.* **158B** 250

[79] Iwasaki Y 1985 *Nucl. Phys.* **B258** 141; 1983 Report UTHEP-118, unpublished

[80] CP-PACS Collaboration (Aoki S et al.) 1999 *Phys. Rev.* **D60** 114508

[81] Sharpe S R 1997 *Phys. Rev.* **D56** 7052; Sharpe S and Shores N 1999, hep-lat/9909090

[82] Golterman M F L and Leung K-C 1998 *Phys. Rev.* **D57** 5703

[83] Bernard C W and Golterman M F L 1994 *Phys. Rev.* **D49** 486

[84] SESAM Collaboration (Eicker N et al.) 1999 *Phys. Rev.* **D59** 014509

[85] UKQCD Collaboration (Allton C R et al.) 1999 *Phys. Rev.* **D60** 034507

[86] UKQCD Collaboration (Garden J et al.) 1999, hep-lat/9909066

[87] CP-PACS Collaboration (Ali Khan A et al.) 1999, hep-lat/9909050

[88] Venkataraman L and Kilcup G 1997, hep-lat/9711006

[89] CP-PACS Collaboration (Ali Khan A et al.) 1999, hep-lat/9909045

[90] SESAM Collaboration (Güsken S et al.) 1999 *Phys. Rev.* **D59** 054504

[91] SESAM Collaboration (Güsken S et al.) 1999 *Phys. Rev.* **D59** 114502

[92] UKQCD Collaboration (Michael C et al.) 1999, hep-lat/9909036

[93] Güsken S 1999, hep-lat/9906034

[94] Drummond I T and Horgan R R 1999 *Phys. Lett.* **B447** 298

[95] SESAM Collaboration (Eicker N et al.) 1996 *Phys. Lett.* **B383** 98

[96] Trottier H D 1999 *Phys. Rev.* **D60** 034506

[97] Tamhankar S and Gottlieb S 1999, hep-lat/9909118

[98] DeTar C, Kaczmarek O, Karsch F and Laermann E 1998 *Phys. Rev.* **D59** 031501

[99] Philipsen O and Wittig H 1998 *Phys. Rev. Lett.* **81** 4056; 1999 *Phys. Lett.* **B451** 146

[100] Knechtli F and Sommer R 1998 *Phys. Lett.* **B440** 345; Knechtli F 1999, hep-lat/9909164

[101] Stephenson P W 1999 *Nucl. Phys.* **B550** 427

[102] DeTar C, Heller U and Lacock P 1999, hep-lat/9909078

[103] Pennanen P, Michael C and Green A M 1999, hep-lat/9908032; Pennanen P 1999, these proceedings

- [104] KTeV Collaboration (Alavi-Harati A et al.) 1999 *Phys. Rev. Lett.* **83** 22; NA48 Collaboration (Fanti V et al.) 1999, hep-ex/9909022
- [105] Leutwyler H 1996 *Phys. Lett.* **B378** 313
- [106] Martinelli G et al. 1995 *Nucl. Phys.* **445** 81
- [107] Lüscher M, Narayanan R, Weisz P and Wolff U 1992 *Nucl. Phys.* **B384** 168
- [108] Sint S 1994 *Nucl. Phys.* **B421** 135; 1995 *Nucl. Phys.* **B451** 416
- [109] Lüscher M 1998, hep-lat/9802029
- [110] ALPHA Collaboration (Capitani S et al.) 1999 *Nucl. Phys.* **B544** 669
- [111] JLQCD Collaboration (Aoki S et al.) 1999 *Phys. Rev. Lett.* **82** 4392
- [112] ALPHA & UKQCD Collaborations (Garden J et al.) 1999, hep-lat/9906013
- [113] Göckeler M et al. 1999, hep-lat/9908005
- [114] Wingate M et al. 1999, hep-lat/9909101
- [115] Sommer R 1994 *Nucl. Phys.* **B411** 839
- [116] ALPHA Collaboration (Guagnelli M et al.) 1998 *Nucl. Phys.* **B535** 389
- [117] Becirevic D, Giménez V, Lubicz V and Martinelli G 1999, hep-lat/9909082
- [118] Becirevic D et al. 1998 *Phys. Lett.* **B444** 401
- [119] SESAM Collaboration (Eicker N et al.) 1997 *Phys. Lett.* **B407** 290
- [120] MILC Collaboration 1999, private communication by C. Bernard
- [121] Ishikawa K, Schierholz G and Teper M 1983 *Z. Phys.* **C19** 327
- [122] Teper M 1998, hep-th/9812187
- [123] Toussaint D 1999, plenary talk presented at *Lattice '99*, hep-lat/9909088
- [124] Morningstar C J and Peardon M 1997 *Phys. Rev.* **D56** 4043; 1999 *Phys. Rev.* **D60** 034509
- [125] UKQCD Collaboration (Bali G et al.) 1993, *Phys. Lett.* **B309** 378
- [126] Vaccarino A and Weingarten D 1999 *Phys. Rev.* **D60** 114501
- [127] Teper M 1997, hep-lat/9711011
- [128] Amsler C and Close F 1996 *Phys. Rev.* **D53** 295
- [129] Weingarten D 1997 *Nucl. Phys. B (Proc. Suppl.)* **53** 232
- [130] Lee W and Weingarten D 1999, hep-lat/9910008
- [131] SESAM & T χ L Collaborations (Bali G et al.) 1997 *Nucl. Phys. B (Proc. Suppl.)* **53** 239; 1998 *Nucl. Phys. B (Proc. Suppl.)* **63** 209
- [132] Thacker B A and Lepage G P 1991 *Phys. Rev.* **D43** 196; Lepage G P et al. 1992 *Phys. Rev.* **D46** 4052
- [133] CP-PACS Collaboration (Manke T et al.) 1999 *Phys. Rev. Lett.* **82** 4396; Manke T 1999, these proceedings
- [134] Juge K J, Kuti J and Morningstar C J 1999 *Phys. Rev. Lett.* **82** 4400
- [135] UKQCD Collaboration (Manke T et al.) 1998 *Phys. Rev.* **D57** 3829
- [136] MILC Collaboration (Bernard C et al.) 1997 *Phys. Rev.* **D56** 7039
- [137] Kuramashi Y 1999, plenary talk presented at *Lattice '99*, hep-lat/9910032
- [138] Martinelli G 1999, plenary talk presented at *Kaon '99*, hep-ph/9910237
- [139] Gupta R, Bhattacharya T and Sharpe S 1997 *Phys. Rev.* **D55** 4036; UKQCD Collaboration (Lellouch L et al.) 1999 *Nucl. Phys. B (Proc. Suppl.)* **73** 312; Allton C et al. 1999 *Phys. Lett.* **B453** 30; JLQCD Collaboration (Aoki S et al.) 1998 *Phys. Rev. Lett.* **81** 1778; 1999 *Phys. Rev.* **D60** 034511
- [140] Hashimoto S 1999, plenary talk presented at *Lattice '99*, hep-lat/9909136
- [141] Shanahan H P 1999, hep-lat/9909052; these proceedings, hep-ph/9909398
- [142] Petronzio R 1999, plenary talk presented at *Lattice '99*
- [143] Guagnelli M, Jansen K and Petronzio R 1999 *Phys. Lett.* **B457** 153; *Phys. Lett.* **B459** 594; *Nucl. Phys.* **B542** 395
- [144] Capitani S et al. 1999, hep-lat/9908011